TEM and STEM analysis on heat-treated and in vitro plasma-sprayed hydroxyapatite/Ti-6Al-4V composite coatings

Dong, Zhili; Khor, Khiam Aik; Quek, C. H.; White, Timothy John; Cheang, P.

2003

Dong, Z. L., Khor, K. A., Quek, C. H., White, T. J., & Cheang, P. (2003). TEM and STEM analysis on heat-treated and in vitro plasma-sprayed hydroxyapatite/Ti-6Al-4V composite coatings. Biomaterials, 24(1), 97-105.

https://hdl.handle.net/10356/95561

https://doi.org/10.1016/S0142-9612(02)00267-3

TEM and STEM analysis on heat-treated and in vitro plasma-sprayed hydroxyapatite/Ti-6Al-4V composite coatings

Z.L. Dong[a], K.A. Khor[b,]*, C.H. Quek[b], T.J. White[a], P. Cheang[c]

[a]Institute of Environmental Science and Engineering (IESE), Nanyang Avenue, Singapore 639798, Singapore

[b]School of Mechanical & Production Enginering, Nanyang Technological University, Nanyang Avenue, Singapore 639798, Singapore

[c]School of Materials Engineering, Nanyang Technological University, Nanyang Avenue, Singapore 639798, Singapore

**Corresponding author.*
E-mail address: mkakhor@ntu.edu.sg (K.A. Khor).

Abstract

A cogent understanding of the microstructure, and indeed nano-structure, of hydroxyapatite (HA) and the interface between Ti-6Al-4V and HA is crucial to its appropriateness as a biomaterials. This paper reports the analysis of plasma-sprayed HA/Ti-6Al-4V composites by transmission electron microscopy (TEM) and scanning transmission electron microscopy (STEM) to elucidate the intricate nature of the materials following plasma spray processing and in vitro evaluation. The novel Ti-6Al-4V/HA composite coating, with approximately 48 wt% HA, had demonstrated attractive tensile adhesion strength (~28 MPa) and improved Young's modulus (~ 55 GPa). Experimental results demonstrated that amorphous calcium phosphate and fine HA grains were formed during rapid splat solidification in the as-sprayed composite coatings. Small Ti-6Al-4V grains were observed adjacent to the amorphous calcium phosphate. The coatings were further heat treated at 600 ℃ for 6 h, and significant crystallisation of the amorphous calcium phosphate phase took place. However, complete crystallisation was not achieved at this temperature, as the coatings invariably contained a small amount of amorphous calcium phosphate phase in some local regions. After immersion in simulated body fluid for 2 weeks and 10 weeks, TEM and STEM confirmed that the interfaces inside the coating maintained good microstructural integrity.

Keywords: Hydroxyapatite; Ti-6Al-4V alloy; Composite; Plasma spraying; Transmission electron microscopy

1. Introduction

Hydroxyapatite (HA), with the chemical formula $Ca_{10}(PO_4)_6(OH)_2$, is one of the most attractive materials for human hard tissue implants because of its close resemblance to chemical composition(Ca/P ratio) of teeth and bones. This promotes rapid bone growth and bonding between bony tissue and implant surfaces. HA has been clinically applied as a dense, sintered material and as

coatings onbioinert metallic implant [1]. As a coating on stems of hip joint prostheses, HA can enhance biological fixation. However, HA coatings with different microstructural characteristics profoundly influence subsequent biological performance, leading to miscellaneous biological responses after implantation [2]. HA coatings have been applied by a wide range of surface deposition techniques including plasma spraying, high-velocity oxy-fuel spraying (HVOF), pulsed laser ablation, ion-beam sputtering, electrophoretic deposition, radio frequency magnetron sputtering, solgel and conventional ceramic processes that involve pressing and sintering [3–13]. Among these techniques thermal spray techniques offer the attractive prospect of economy and efficient deposition of HA [1].

HA is known for its good biocompatibility. However, a major drawback is its relatively poor mechanical properties compared to natural bone, making it unsuitable for high-load applications. Its fracture toughness is only about 1 $MPam^{1/2}$. In order to achieve the mechanical characteristics needed for biomedical applications, blending with a tough phase is essential. Titanium metal, Ti-6Al-4V alloy, yttria-stabilised zirconia (YSZ), Ni_3Al and Al_2O_3 ceramics have been considered good candidates as the reinforcing phases [14–17]. The mechanical properties of such HA-based composites are strongly dependent on the reinforcement fillers and interfacial adhesion.

In a previous study, HA and HA/Ti-6Al-4V composite coatings were fabricated by plasma spraying and characterised by X-ray diffraction (XRD) and scanning electron microscopy (SEM) [18]. The present investigation focuses on reinforcing HA coatings with a tough secondary phase. The toughening material chosen was Ti-6Al-4V alloy. The reasons for this are as follows: (1) The melting point of Ti-6Al-4V is comparable to that of HA, thereby ensuring homogeneous melting of the composite during plasma spraying, and further enhancing the bonding between HA and Ti-6Al-4V lamellae due to more complete wetting in the molten state. This yields a strong composite coating. (2) Bonding strength between the coating and substrate can be improved as Ti-6Al-4V lamellae in the coating can adhere to implant substrate material—Ti-6Al-4V strongly. (3) Ti-6Al4V+HA composites exhibit high bioactivity when an HA outer layer is present. When multi-layered functionally graded materials (FGM) are fabricated by varying the proportion of Ti-6Al-4V during plasma spraying, a pure HA coating on the outer surface of the FGM displays bioactivity equivalent to single-layer HA coatings. (4) Ti-6Al-4V is relatively stable in body fluids and has a low density.

As Ti-6Al-4V alloys and plasma-sprayed HA coatings have been well studied, the present investigation focused on plasma-sprayed Ti-6Al-4V/HA composite layer. With the aid of TEM, and STEM phase distributions in the coatings and metallic/ceramic interfaces were characterised, especially with respect to the influence of heat treatment and in vitro immersion duration.

2. Experimental materials and procedures

The HA/Ti-6Al-4V composite powders used for deposition were synthesised from pure HA material and Ti-6Al-4V alloy. As described in a previous report [19,20], HA raw material was produced using a wet chemical method, i.e. having 0.5 M calcium hydroxide to react with 0.3 M orthophosphoric acid in a temperature-controlled bath. The resultant precipitate was dried at 180 ℃, followed by calcination at 800 ℃ for 4 h. Commercially available Ti-6Al-4V powder of —100 mesh with a particle size range 53–75 μm (Micron Co., Canada) was used. Coating HA slurry onto Ti-6Al-4V granules as described elsewhere [19] yielded Ti-6Al-4V/ HA composite powders with particle size in the range of 75–106μm. The average proportion of the HA in the composite powders is ~48 wt%.

A computerised plasma spraying system 4500 (Praxair Thermal Inc., USA) was used for coating deposition. Before plasma spraying, the Ti-6Al-4Vsubstrates were sandblasted with − 24 mesh alumina grit. The plasma spray parameters are listed in Table 1. The ~100 μm thick coatings were heat

treated at 600 ℃ for 6 h to speed up the re-crystallisation process and to release thermal residual stresses. Coatings for bond strength measurement were sprayed onto cylinders of 25-mm in diameter and height. Bond strengths were measured according to the ASTM standard C633-79. Two identical cylindrical nickel stubs were used as a set, one with the coating on the surface and the other without. A high performance DP-460 Epoxy Adhesive (3M, USA) with a maximum bond strength of 40 MPa was used to join the two stubs. The surface of the uncoated stubs was sandblasted to enhance the adhesion strength. The two stubs were aligned and a weight of about 420 g was applied to ensure intimate contact between the two surfaces. After 12 h of curing at room temperature, the bond strength was measured using an Instron 4302 tester at a crosshead speed of 1 mm min^{-1}.

XRD, SEM, and TEM examined the resultant coatings. TEM specimens were prepared by grinding the coatings to less than 50 μm with emery paper followed by thinning with a Gatan precision ion-polishing machine. Cross-sectional TEM specimens from the coatings were prepared using a method similar to that described by Unal et al. [21]. A JEOL JEM3010 TEM operated at 300 kV was used to characterise the microstructure/nanostructure of the composite coatings.

The simulated body fluid (SBF) was prepared in accordance to the formulation of Kokubo et al. [22]. The concocted fluid had an ionic concentration that closely resembles the concentration of human blood plasma, as shown in Table 2. The resultant composition was buffered to a physiological pH of 7.25 at 36.5 ℃ with tris(hydroxymethyl)-aminomethane and hydrochloric acid (HCl). The coated samples (both as-sprayed and heat-treated) were immersed in sealed SBF-containing vials for time periods of 2, 4, 6, 8 and 10 weeks. The whole experiment was performed in a laboratory constant temperature water bath maintained at a temperature of 36.5±0.1 ℃ and subjected to a constant stirring and gentle shaking motion.

3. Results

3.1. TEM observation of as-sprayed HA/Ti-6Al-4V composite

Thermal spraying is a unique process to rapidly fabricate layered coating structures. Thermal sprayed coatings are built up by microscaled molten splat solidification. Occasionally, some unmelted particles are captured by the successive droplets arriving on the substrate and get embedded in the subsequent layered structures. Pores are formed during solidification due to both shrinkage and air entrapment. In this HA/Ti-6Al-4V composite coating system, SEM images from polished cross-sections clearly demonstrated the Ti-6Al-4V and HA phases layered in an alternating pattern (Fig. 1). XRD revealed that as-sprayed HA coatings contain a large amount of amorphous calcium phosphate phase (Fig. 2). Among the crystalline phases, the major one is HA. Minor amounts of CaO as well as $Ca_3(PO_4)_2$ (TCP) and $Ca_4P_2O_9$ (TTCP) exist in the coating due to the decomposition of HA during the high-temperature spray process.

In order to clarify the nano-scale phase morphology and interface structure, the present study emphasized TEM and STEM analyses. In particular, bright field images and selected area electron diffraction patterns revealed detailed phase distributions in the HA/Ti-6Al-4Vcomposite coating. Fig. 3 shows a typical TEM HA/ Ti-6Al-4V coating structure, where fine HA crystalline material is distributed through an amorphous matrix, which also encapsulates Ti-6Al-4V crystals. The amorphous calcium phosphate phase existed almost ubiquitously in the as-sprayed coating.

Regions containing mainly Ti-6Al-4V material were also studied as shown in Fig. 4. The selected area diffraction (SAD) pattern also shows very faint spots associated with HA crystals. Regions containing HA and amorphous phase is shown in a higher magnification TEM image (Fig.

5). Such amorphous phase that exists in the as-sprayed coatings can be mostly transformed into the crystalline HA phase through post-spray heat treatment.

As expected, the microstructures of HA/Ti-6Al-4V composite coatings are more convoluted when compared to pure HA coatings due to the presence of both ceramic and metallic phases in the starting powders. The composite powders before plasma spraying contained α' Ti-6Al-4V and pure HA phases, as confirmed by the XRD patterns. As an artifact of the preparation procedure, typical powder particle structure shows a large Ti-6Al-4V core rimmed by a homogeneous HA layer [19]. Such structures inhibit a lower incidence of Ti-6Al-4V oxidation during plasma spraying because of the HA passivation role. According to the STEM/EDX results, it was found that the metallic phase and ceramic overlayer were intimately contacted which facilitates diffusion and exchange of elements (Fig. 6), particularly from metallic region to ceramic region.

In many cases, no clear interface could be detected between metallic and ceramic structure in TEM as the wetting enhanced diffusion between them in the molten state during plasma spraying. Rapid solidification induced the formation of fine grains, or even amorphous calcium phosphate, that was unable to crystallise within a short duration at the crystallisation temperature employed in this study.

3.2.Influence of the post-spray heat treatment on microstructure and properties of HA/Ti-6Al-4V composite coating

The biodegradation of HA coating over time depends largely on the degree of crystallinity of HA [1]. Fast cooling enhances the formation of the amorphous phase. One purpose of post-spray heattreatment was to promote crystallisation, as amorphous materials are more readily resorbed by body fluid, hence weakening the interface between coating and implant. Controlled post-spray heat treatment, e.g. 600 ℃ for 6 h effectively preferentially transforms the amorphous calciumphosphate into HA, rather than other phosphates. The XRD result showed that the quantity of HA increased significantly after heat treatment, while α-tricalcium phosphate, β-tricalcium phosphate, tetracalcium phosphate, and CaO phases were almost undetectable [19]. TEM micrographs showed more crystalline HA grown from amorphous regions (see Fig. 7) in the treated samples.

The Ti-6Al-4V fine grains formed during plasma spray were relatively stable during the heat treatment, as little grain growth was observed. The fine grains after heat treatment were around 50 nm or even smaller (Fig. 8). A small amount of amorphous phase was observed in some local areas, as the phase transformation from amorphous into HA was not 100%, even after long duration high-temperature treatment (Fig. 9).

In many cases, larger grains of HA were observed after heat treatment as shown in Fig. 10 with the grain size of about 100 nm or larger. It was believed that heat treatment at even higher temperature could lead to microstructure changes in substrate material. However, such conditions have been employed in the present study. Another method to avoid damage on substrate materials whilst accomplishing phase transformation of the amorphous calcium phosphate to HA is by laser surface heat treatment [23].

Compared with pure HA, the addition of Ti-6Al-4V alloy to HA greatly increased the mechanical properties of the coating both prior to, and after heat treatment [19]. Bond strengths of the Ti-6Al-4V/HA composite coating materials on Ti-6Al-4V substrate, as tested according to ASTM C-633 procedure are at a range ~23–28 MPa. This range of values are almost double that of a pure HA coating (~10–15MPa).

The Ti-6Al-4V/HA composite coatings were immersed into SBF in the range 2–10 weeks to determine the microstructure changes that would influence the performance of the material. It was found on the inside the coating did not undergo obvious changes, although some HA crystals in some regions appears to have coarsened (Figs. 11 and 12). The interface between ceramic and metallic phases evidently maintained decent integrity following the SBF test, even after 10 weeks immersion.

4. Discussion

Based on the present analytical TEM study and previous SEM and XRD examination, the microstructure characteristics of this HA/Ti-6Al-4V bioactive coating system were studied. Both ceramic/ceramic and ceramic/metallic interfaces in the HA/Ti-6Al-4V composite coating system are found to be strongly adhesive in the as-sprayed conditions. No cracks or separation between the different materials were observed by TEM (see Fig. 6). This is attributed as asignificant factor for the enhanced cohesive and adhesive strength of the coating. The average tensile bond strength value of the 50 wt% Ti-6Al-4V/50 wt% HA system was found to be 28 MPa (5 data points). This is almost twice the value obtained for typical plasma-sprayed HA coating (15 MPa). In addition, the existence of ductile Ti-6Al-4V retards crack propagation in the coating and therefore contributes to the general fracture toughness of the composite coating.

It is also accepted that post-spray heat treatment can promote interfacial bondings, and transform the amorphous calcium phosphate into HA crystals, thereby enhancing both the mechanical properties and biocompatibility of the coatings.

The heat treatment temperature and treatment duration were selected primarily on the basis of maximising HA formation from amorphous calcium phosphate [19], while avoiding alteration of the substrate. Although it is generally accepted that higher temperatures can help hasten the amorphous→crystalline phase transformation, it is practical to use lower heat-treatment temperatures to avoid serious irreversible structural and property changes to the Ti-6Al-4V substrate. In the present study 600 ℃, 6h seem to be ideal as almost complete crystallisation of HA was achieved with any evidence of oxidation to the Ti phase.

These results suggest that HA/Ti-6Al-4V composite materials prepared by plasma spraying can be used as bond coat layer between Ti-6Al-4V implant and HA coating. TEM examination has proven that the coating structure is relatively stable in the SBF. Interfaces inside the coating show good adhesion. Detailed in vitro and in vivo trials are still going on. The results will be reported in future publications.

5. Conclusions

The microstructure of plasma-sprayed HA/Ti-6Al-4V composite material was investigated using analytical transmission electron microscopy (TEM) and scanning transmission electron microscopy (STEM). The composite was a dense-layered structure, containing HA, finely divided Ti-6Al-4V and amorphous calcium phosphate. Adhesive ceramic/ceramic and ceramic/metallic interfaces were observed before and after heat treatment. After heat treatment at 600 ℃ for 6 h, the amorphous calcium phosphate was transformed into fine HA crystals with minimal decomposition. Localised retention of amorphous phase was found in the heat-treated sample. This indicates that certain ‘stabilising’ factors could exist in the system that prevents a complete conversion to HA. The fine Ti-6Al-4V grains are stable and do not coarsen into large grains, which will compromise the mechanical properties of the composites.

The high bond strength of HA/Ti-6Al-4V was attributed to the good adhesion among the interfaces

between HA and Ti-6Al-4V as evident in the TEM micrographs. Heat treatment at 600 ℃, 6 h is apparently suitable for this composite system and has minimal influence on the substrate than that might be expected if higher temperature heat treatments were employed. Crystallisation of amorphous calcium phosphate to HA was evident and this augured well for the biomechanical integrity of this composite system in vivo.

Microstructure of this composite coating undergoes minor changes after a short period (2–10 weeks) of SBF test. However, no apparent changes in the Ti-6Al-4V/ HA interface microstructure was observed even after 10 weeks of immersion in the SBF. This indicates that the plasma-sprayed Ti-6Al-4V/HA composite is stable in the SBF and would maintain its post-implantation biocompatible and bioactive properties.

Acknowledgements

The authors would like to thank Nanyang Technological University for supporting this research project in the form of research grant JT ARC 4/96.

References

[1] Hench LL. Bioceramics. J Am Ceram Soc 1998;81:1705–28.

[2] Wang BC, Chang E, Yang CY, Tu D, Tsai CH. Characteristics and osteoconductivity of three different plasma-sprayed hydroxyapatite coatings. Surf Coat Technol 1993;58:107–17.

[3] Haman JD, Boulware AA, Lucas LC, Crawmer DE. High-velocity oxyfuel thermal spray coatings for biomedical applications. J Thermal Spray Technol 1995;4:179–84.

[4] Kyeck S, Remer P. Realisation of graded coatings for biomedical use. Mater Sci Forum 1999;308–311:368–73.

[5] Singh RK, Qian F, Damodaran R, Moudgil S. Laser deposition of hydroxyapatite coatings. Mater Manuf Processes 1996;11: 481–90.

[6] Ong JL, Harris LA, Lucas LC, Lacefield WR, Rigney D. X-ray photoelectron spectroscopy characterization of ion-beam sputter-deposited calcium phosphate coatings. J Am Ceram Soc 1991;74:2301–4.

[7] Dasarathy H, Riley C, Coble HD, Lacefield WR, Maybee G. Hydroxyapatite/metal composite coatings formed by electrocodeposition. J Biomed Mater Res 1996;31:81–9.

[8] Wolke JGC, van Dijk K, Schaeken HG, de Groot K, Tansen JA. Study of the surface characteristics of magnetron-sputter calcium phosphate coatings. J Biomed Mater Res 1994;28:1477–84.

[9] Yamashita K, Yagi T, Umegaki T. Bonelike coatings onto ceramics by reactive magnetron sputtering. J Am Ceram Soc 1996;79:3313–6.

[10] Montenero A, Gnappi G, Ferrari F, Cesari M, Salvioli E, Mattogno L, Kaciulis S, Fini M. Sol–gel derived hydroxyapatite coatings on titanium substrate. J Mater Sci 2000;35:2791–7.

[11] Haddow DB, James PF, Van Noort R. Sol–gel calcium phosphate coatings for biomedical applications. J Sol–Gel SciTechnol 1998;13:261–5.

[12] Jillavenkatesa A, CondrateSr RA. Sol–gel processing of hydroxyapatite. J Mater Sci 1998;33:4111–9.

[13] Hero H, Wie L, Jorgensen RB, Ruyter IE. Hydroxyapatite coatings on Ti produced by hot isostatic pressing. J Biomed Mater Res 1994;28:343–8.

[14] Chang E, Chang WJ, Wang BC, Yang CY. Plasma spraying of zirconia-reinforced hydroxyapatite composite coatings on titanium. J Mater Sci: Mater Med 1997;8:193–200.

[15] Bishop A, Lin CY, Navaratnam M, Rawlings RD, McShane HB. A functionally gradient material produced by a powder metallurgical process. J Mater SciLett 1993;12:1516–8.

[16] Choi JW, Kong YM, Kim HE. Reinforcement of hydroxyapatite bioceramic by addition of Ni_3Al and Al_2O_3. J Am Ceram Soc 1998;81:1743–8.

[17] Kong YM, Kim S, Kim HE. Reinforcement of hydroxyapatite bioceramic by addition of ZrO2 coated with Al_2O_3. J Am Ceram Soc 1999;82:2963–8.

[18] Khor KA, Cheang P, Wang Y. The thermal spray processing of HA powders and coatings. J Med 1997;49:51–7.

[19] Quek CH. Masters of engineering thesis. Singapore: Nanyang Technological University, 1999.

[20] Khor KA, Dong ZL, Quek CH, Cheang P. Microstructure investigation of plasma sprayed HA/Ti6Al4V composites by TEM. Mater SciEng-A, 2000;281:221–8.

[21] Unal O, Heuer AH, Mitchell TE. Preparation of cross-sectional specimens of ceramic thermal barrier coatings for transmission electron microscopy. J Electron Micro Technol 1990;14:307–12.

[22] Kokubo T. In: Yamamuro T, Hench LL, Wilson J, editors. CRC handbook of bioactive ceramics., Vol. 1. Boca Raton, FL: CRC Press, 1990. p. 41–9.

[23] Ranz X, Pawlowski L, Sabatier L, Fabbro R, Aslanian T. Phase transformations in laser treated hydroxyapatite coatings. Proceedings of the 15th International Thermal Spray Conference, May 1998, Nice, France, p. 1343–49.

List of Tables

List of Figures

Plasma gas	Argon: 1.85 $m^3 h^{-1}$
Auxiliary gas	Helium: 1.64 $m^3 h^{-1}$
Carrier gas	Argon: 0.30 $m^3 h^{-1}$
Net energy	12 kW
Gun current	600–1000 A
Gun transverse speed	0.25 $m s^{-1}$
Stand-off distance	0.08–0.14 m
Powder feedrate	0.01 $kg min^{-1}$

Table 1

Ionic species	Ionic concentrations (mM)	
	Blood plasma	Formulated SBF
Calcium (Ca^{2+})	2.5	2.2
Hydrogen phosphate (HPO_4^{2-})	1.0	0.8
Sodium (Na^{+})	142.0	140.3
Chloride (Cl^{-})	148.8	148.0
Magnesium (Mg^{2+})	1.5	1.3
Potassium (K^{+})	5.0	5.3
Hydrogen carbonate (HCO_3^{-})	4.2	4.0

Table 2

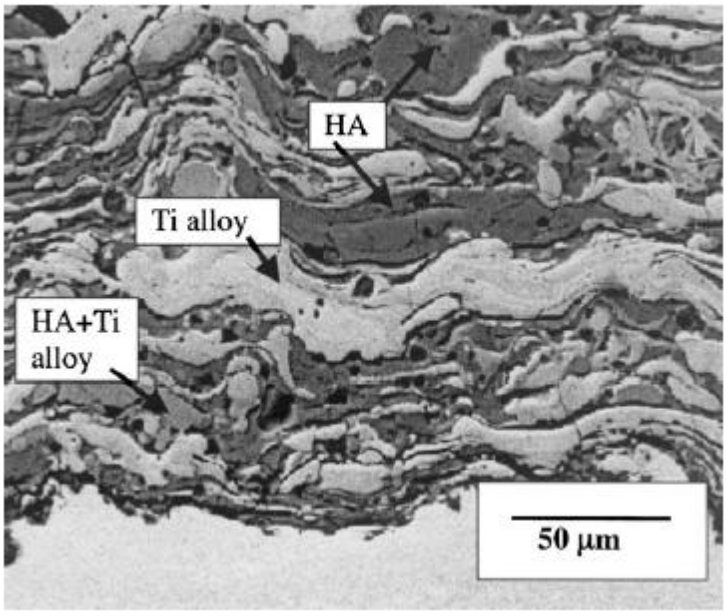

Figure 1

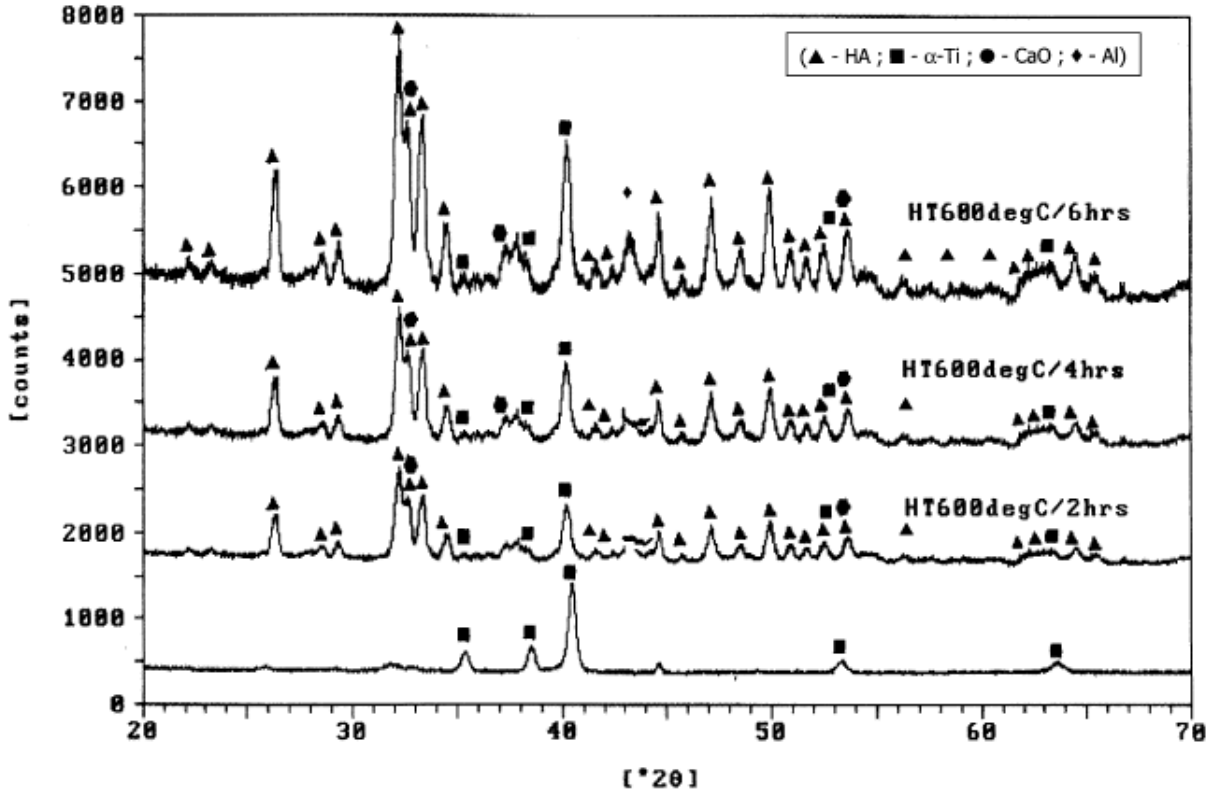
(▲ - HA ; ■ - α-Ti ; ● - CaO ; ♦ - Al)
HT600degC/6hrs
HT600degC/4hrs
HT600degC/2hrs
[counts]
[°2θ]
8000
7000
6000
5000
4000
3000
2000
1000
0
20
30
40
50
60
70

Figure 2

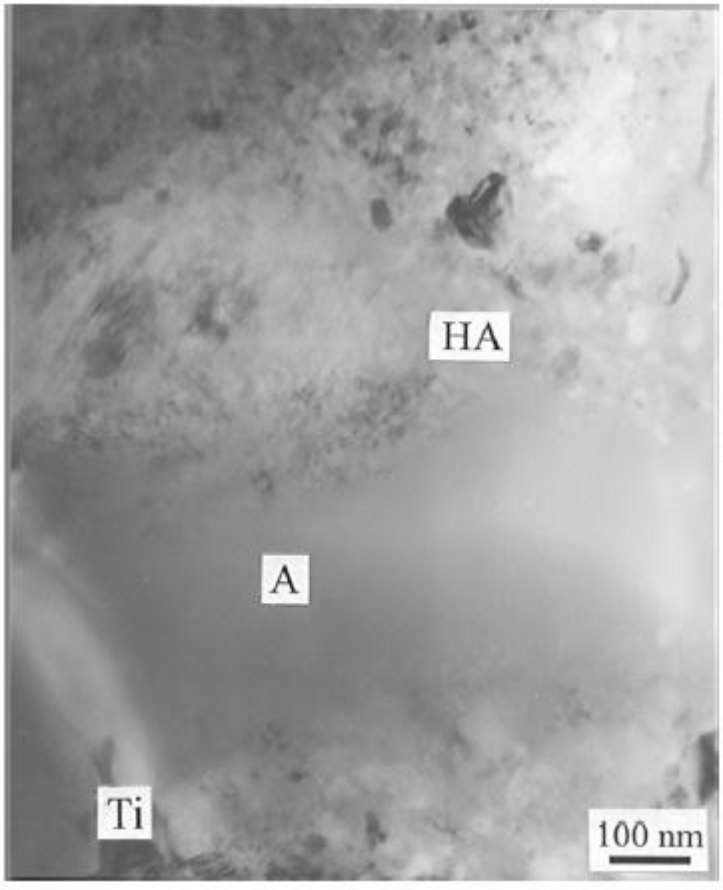

Figure 3

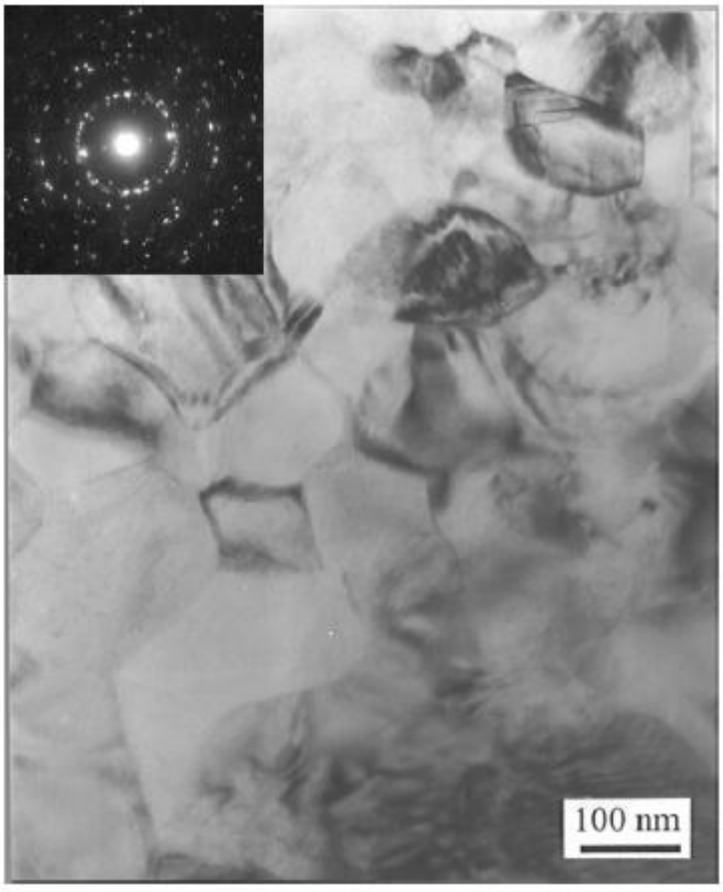

Figure 4

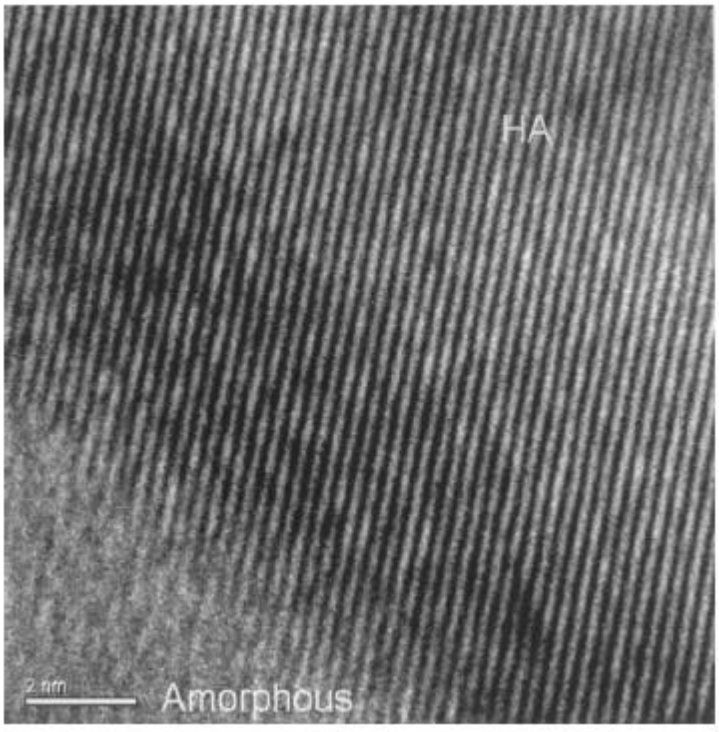

Figure 5

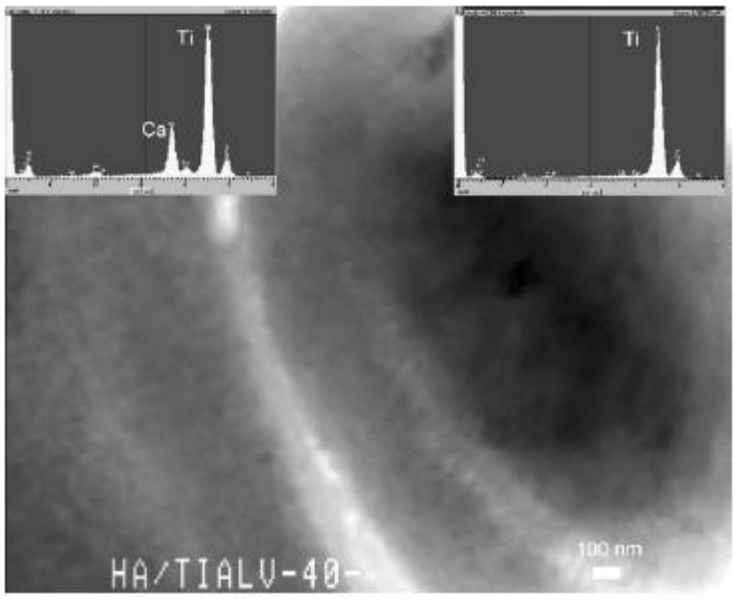

Figure 6

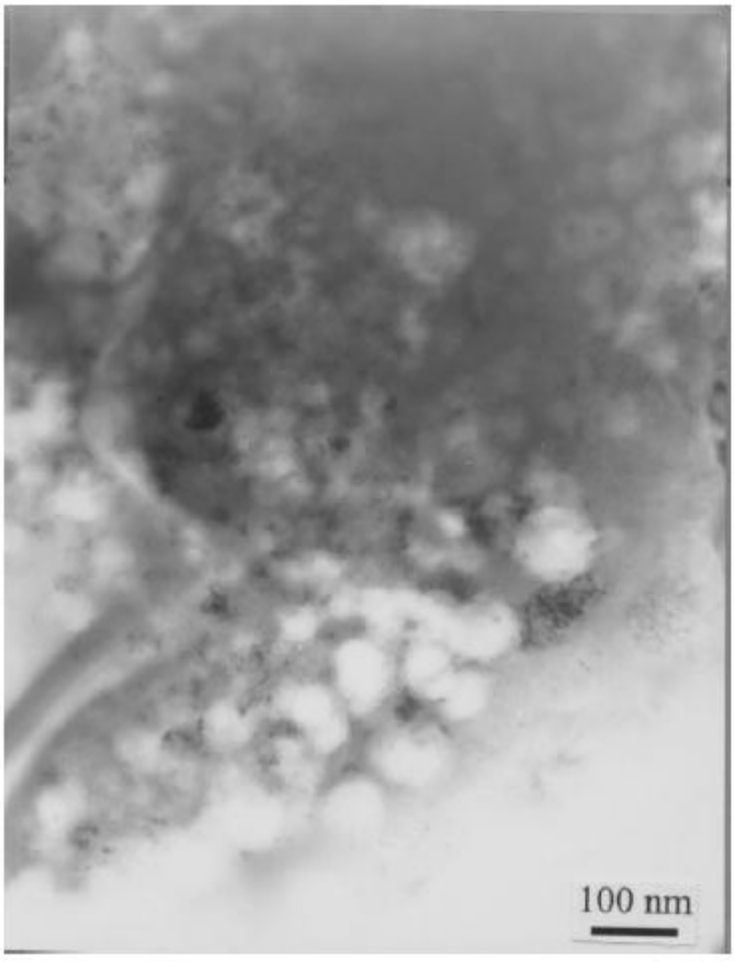

Figure 7

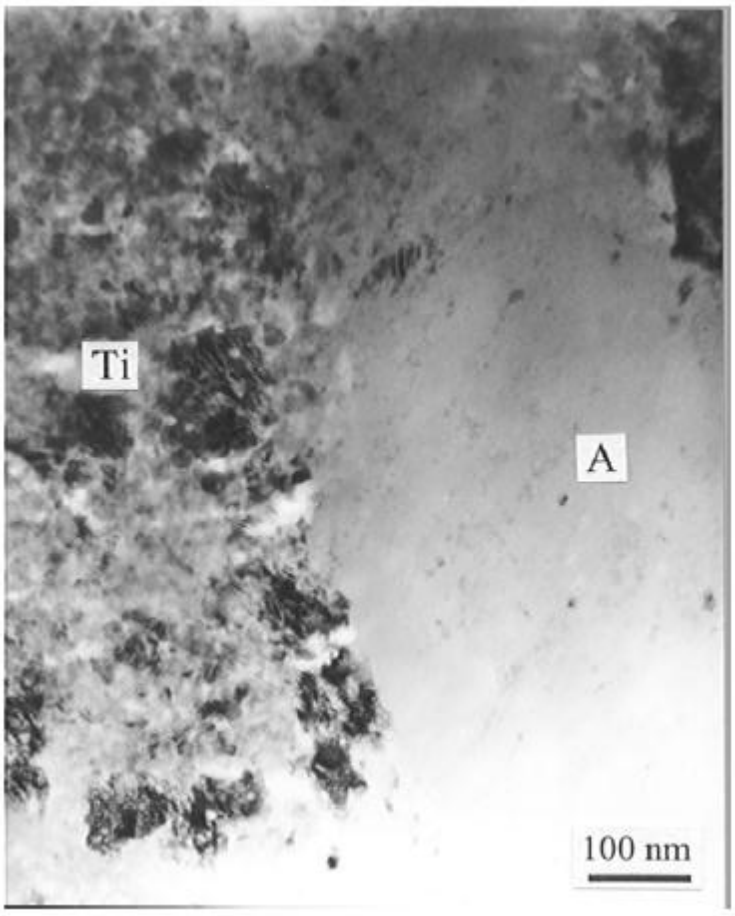

Figure 8

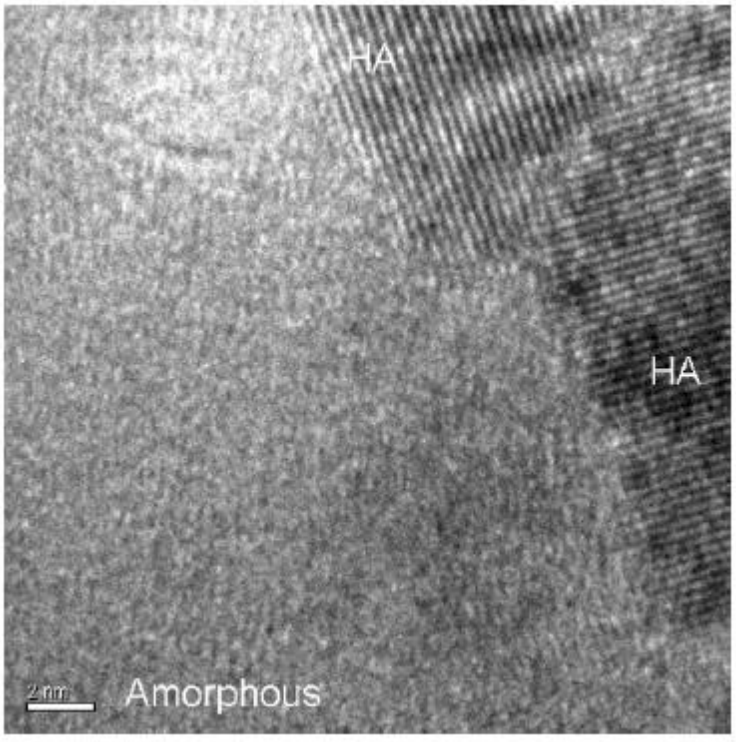

Figure 9

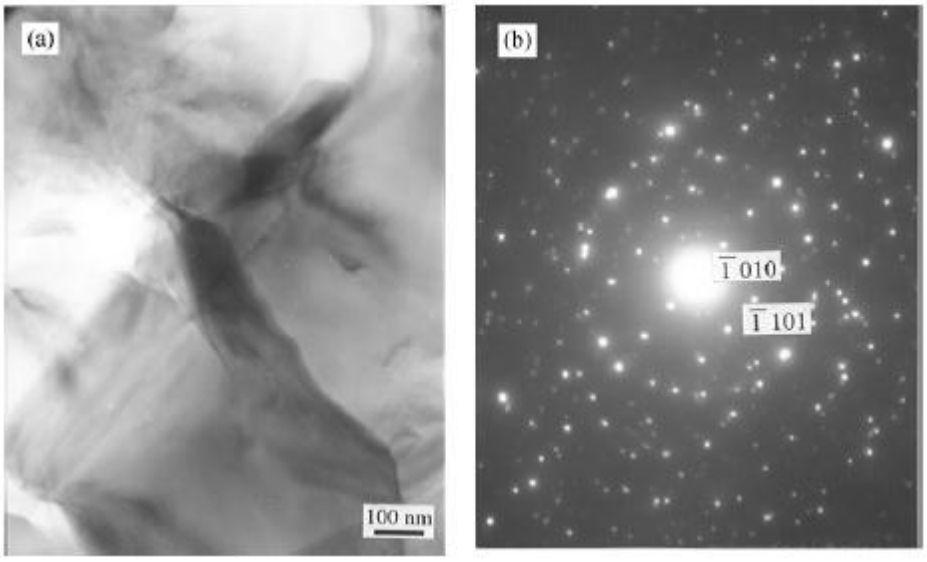

Figure 10

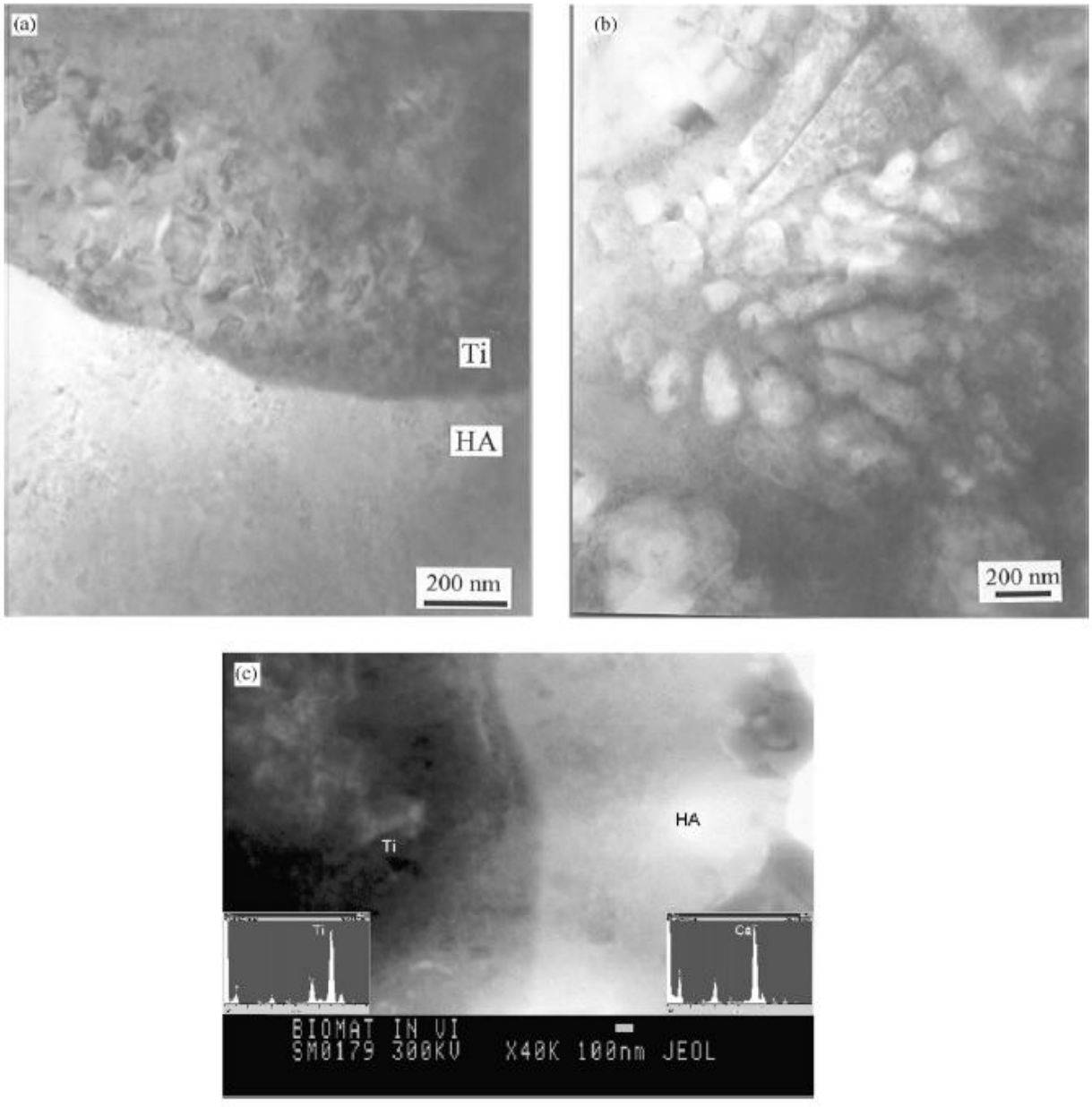
(a)
Ti
HA
200 nm
(b)
200 nm
(c)
Ti
HA
Ti
Ca
BIOMAT IN VI
SM0179 300kV X40K 100nm JEOL

Figure 11

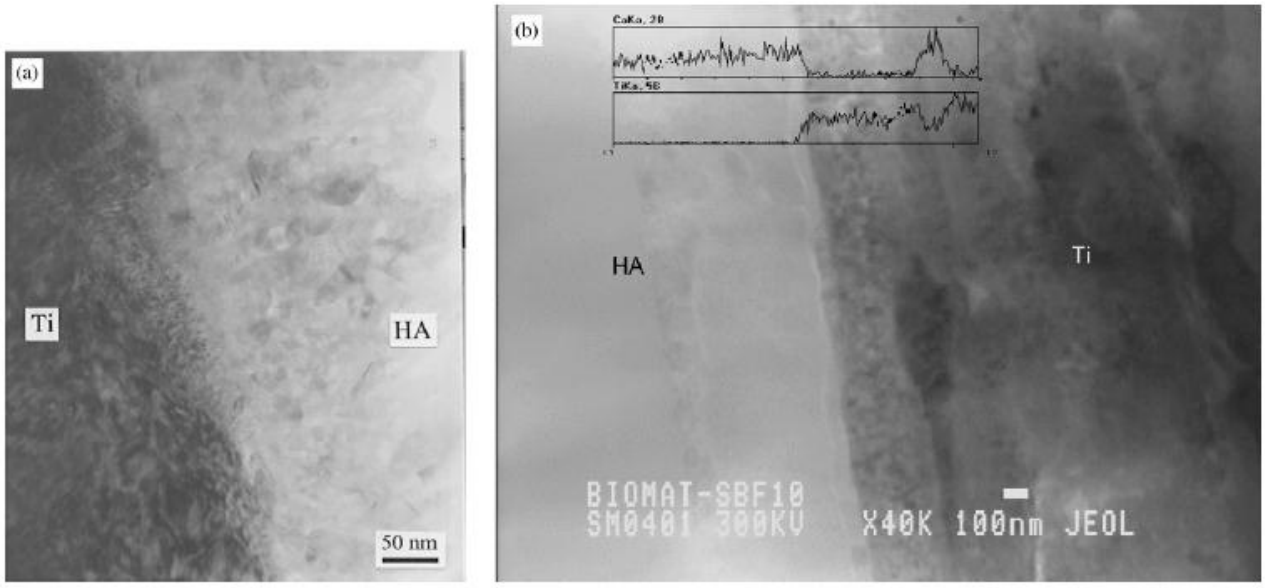
(a)
Ti
HA
50 nm
(b)
CaKa, 2D
TiKa, 5B
HA
Ti
BIOMAT-SBF10
SM0401 300KV
X40K 100nm JEOL

Figure 12